Generation of exchange flows in estuaries by tidal and gravitational eddy viscosity-shear covariance (ESCO)

Dijkstra, Yoeri M.; Schuttelaars, Henk M.; Burchard, Hans

DOI
10.1002/2016JC012379

Publication date
2017

Document Version
Final published version

Published in
Journal Of Geophysical Research-Oceans

AGU PUBLICATIONS

JGR

Journal of Geophysical Research: Oceans

RESEARCH ARTICLE

10.1002/2016JC012379

Generation of exchange flows in estuaries by tidal and gravitational eddy viscosity-shear covariance (ESCO)

Yoeri M. Dijkstra[1,2], Henk M. Schuttelaars[1], and Hans Burchard[3]

[1]Delft Institute of Applied Mathematics, Delft University of Technology, Delft, Netherlands, [2]Deltares, Delft, Netherlands, [3]Leibniz Institute for Baltic Sea Research Warnemünde, Rostock, Germany

Key Points:
- We generalize and further systematize theory on exchange flows through eddy viscosity-shear covariance (ESCO)
- We identify a new exchange flow contribution due to gravitational eddy viscosity-shear covariance (g-ESCO)
- g-ESCO is typically of a similar importance as gravitational circulation and tidal ESCO (previously also called tidal straining circulation)

Correspondence to:
Y. Dijkstra,
y.m.dijkstra@tudelft.nl

Citation:
Dijkstra, Y. M., H. M. Schuttelaars, and H. Burchard (2017), Generation of exchange flows in estuaries by tidal and gravitational eddy viscosity-shear covariance (ESCO), *J. Geophys. Res. Oceans*, *122*, 4217–4237, doi:10.1002/2016JC012379.

Received 28 SEP 2016
Accepted 16 MAR 2017
Accepted article online 20 MAR 2017
Published online 22 MAY 2017

Abstract We present a systematic analysis of generation mechanisms for exchange flows in partially stratified estuaries using water column (1DV) and width-averaged (2DV) numerical models. We focus on exchange flows generated by eddy viscosity-shear covariance (ESCO). We identify two distinctly different physical mechanisms. The first, tidal ESCO circulation, results from interactions between the barotropic tide and temporal variations of the eddy viscosity. While this flow is mostly generated by direct interactions between the tide and eddy viscosity variations at the main tidal frequency, a similarly important contribution can be attributed to indirect interactions. These are more complex interactions involving eddy viscosity variations at other frequencies than the main tidal frequency (e.g., M_4). The second mechanism is called gravitational ESCO circulation. This results from an amplification of the gravitational circulation through indirect interactions between the gravitational circulation and temporal variations of the eddy viscosity at any time scale. Tidal and gravitational ESCO circulations are generated by different mechanisms and have a different dependency on the phase and frequency of eddy viscosity variations and the density gradient. The relative contributions of gravitational circulation and tidal and gravitational ESCO circulation to the exchange flow are typically 1/3 each in tidally energetic well-mixed or partially stratified estuaries. The results are generalized using an idealized width-averaged model of the Scheldt River estuary. This model confirms the results of the water column model and additionally shows that temporal variations of turbulence not captured in the water column model have a significant effect on the exchange flow.

1. Introduction

The exchange flow is an important contributor to the net transport of salt, suspended sediments, and dissolved substances in estuaries [see e.g., *Geyer and MacCready*, 2014]. This flow, also called estuarine circulation, is a subtidal or residual flow, with root-mean-square velocities which are generally an order of magnitude smaller than the tidal flow in tidally energetic estuaries. Since no precise agreed definition exists, we define the exchange flow here as the contribution to the subtidal flow that has a cross-sectional average of zero. In most midlatitude estuaries, the exchange flow velocity is directed up-estuary near the bed and down-estuary near the surface.

In what *Geyer and MacCready* [2014] call the classical theories, the estuarine circulation consists of the gravitational circulation and the shear due to the river discharge [*Pritchard*, 1956; *Hansen and Rattray*, 1965; *Chatwin*, 1976; *MacCready*, 2004]. Gravitational circulation is created by the balance of a baroclinic pressure gradient induced by an along-estuary density gradient and a subtidal barotropic pressure gradient. Later, other mechanisms contributing to the along-channel estuarine circulation were identified. These mechanisms include lateral advection [*Fischer*, 1972; *Lerczak and Geyer*, 2004; *Burchard and Schuttelaars*, 2012; *Schulz et al*., 2015], longitudinal advection [*Li and O'Donnell*, 2005], wind stress [*Scully et al*., 2005; *Burchard*, 2009], wind induced density straining [*Burchard and Hetland*, 2010], Earth's rotation [*Lerczak and Geyer*, 2004; *Huijts et al*., 2006], and flow curvature [*Chant*, 2002].

The focus of this paper is the exchange flow contribution induced by the covariance between the eddy viscosity and velocity shear variations on the tidal time scale [*Jay and Musiak*, 1994]. This exchange flow is the tidal average of the time-varying deformation of the velocity profile caused by time variations of the eddy viscosity. This contribution has been called straining circulation [*Burchard et al*., 2011; *Geyer and MacCready*, 2014] or exchange flow induced by asymmetric turbulent mixing (ATM) [*Cheng et al*., 2011, 2013]. It will be

demonstrated in this paper that both these names are not sufficiently accurate. Therefore, we introduce the name *eddy viscosity-shear covariance circulation* or ESCO circulation.

One of the important physical mechanisms causing variations of the eddy viscosity associated with ESCO circulation is strain-induced periodic stratification (SIPS) [*Van Aken*, 1986; *Simpson et al*., 1990]. Restricting our attention to stratification by salinity, SIPS describes a process where the vertical profile of the tidal velocity strains the salinity profile. During flood, this leads to a tendency of dense sea water to move over less salty water, leading to an increase in turbulent kinetic energy (TKE). Conversely, the ebb velocity advects less salty water over sea water leading to a stably stratified water column and a reduction of TKE. As a result, the eddy viscosity varies on the M_2 tidal time scale assuming the M_2 tide is the main tidal constituent. This process has been verified from observations by e.g., *Peters* [1999], *Geyer et al*. [2000], *Rippeth et al*. [2001], *Stacey and Ralston* [2005], and *Simpson et al*. [2005] and numerical models by e.g., *Simpson et al*. [2002], *De Boer et al*. [2008], and *Verspecht et al*. [2009].

Apart from SIPS, there are many other mechanisms that lead to temporal variations of TKE. Examples of mechanisms that induce variations of turbulence on an M_2 tidal time scale are asymmetric shear, tidal asymmetry, and depth asymmetry. Asymmetric shear denotes a difference in the shape of the vertical velocity profiles during ebb and flood. The combination of an M_2 tidal flow and an exchange flow for example leads to a different degree of velocity shear during ebb and flood and therefore to a variation in TKE production [*Burchard and Hetland*, 2010]. Tidal asymmetry relates not to an asymmetry in shape, but in magnitude of the velocity between ebb and flood. This leads to a temporal variation in TKE production. TKE production additionally scales with the water depth. A water level difference between ebb and flood, i.e., depth asymmetry, therefore results in temporal variations in TKE production. Apart from M_2 variations in TKE production, these mechanisms also generate TKE variations on other frequencies, such as the M_4 component. Another source of TKE variations on the M_4 frequency is the M_2 tide itself. Tidal velocity variations produce less turbulent energy during the slack tides than during the peak tides. These variations result in time variations of TKE with a predominant M_4 component, which can be of the same order of magnitude as the tidally averaged TKE.

The work of *Stacey et al*. [2008], *Burchard and Hetland* [2010], and *Cheng et al*. [2010, 2011, 2013] has provided us with much of our insight into the ESCO circulation. Using an idealized one-dimensional model, *Stacey et al*. [2008] showed that the absolute magnitude of the ESCO circulation depends strongly on the moment during which the water column stratifies. Using a nonlinear one-dimensional vertical model coupled to a $k-\varepsilon$ turbulence model, *Burchard and Hetland* [2010] found that the ESCO circulation is a factor two larger than the gravitational circulation in the parameter space associated with well-mixed and partially stratified estuaries. *Burchard and Hetland* [2010] additionally establish that the ESCO circulation scales approximately linearly with the salinity gradient, similar to the gravitational circulation. *Cheng et al*. [2010] used a two-dimensional longitudinal-vertical perturbation approach, assuming that the time-varying eddy viscosity is small compared to the tidal-mean eddy viscosity, which is typical for well-mixed systems. They found that the resulting ESCO circulation is typically of the same order of magnitude as the gravitational circulation. They also observe that ESCO circulation does not only scale with eddy viscosity variations but also scale with the magnitude of the tidal velocity. *Cheng et al*. [2011, 2013] extend this to partially and strongly stratified estuaries using a combination of a fully numerical model and a perturbation approach. They showed that the level of stratification strongly affects the vertical structure, direction, and magnitude of the ESCO circulation. From these studies, it follows that ESCO circulation is a complex process that depends on multiple variables and multiple physical mechanisms, which have not been completely identified.

Hence, the aim of this paper is to identify the mechanisms resulting in ESCO circulation, their relative importance and their sensitivity to flow parameters. We will show that, in a 1DV context, the ESCO circulation as identified by *Burchard and Hetland* [2010] and *Cheng et al*. [2011, 2013] is actually made up of two different physical mechanisms with a clearly distinct behavior. This observation will then be used to develop a generalized theoretical framework for ESCO circulation. To identify the different mechanisms, we will use a one-dimensional (1DV) and two-dimensional width-averaged (2DV) model with a $k-\varepsilon$ turbulence closure. The 1DV model is applied to a wide parameter space that covers parameter values found in well mixed to partially stratified estuarine conditions. For the 1DV simulations, we will restrict our attention to the baroclinic and barotropic tidal forcing and do not take the effects of the Earth's rotation (Coriolis) or wind into account. Similarly, we ignore the effects of geometry, bathymetry, advection, and river discharge. These

restrictions are severe in the context of real estuaries but allow us to identify the mechanisms resulting in ESCO circulation as clearly as possible. The 2DV model generalizes the 1DV theory using a case study, which includes the effects of geometry, bathymetry, advection, and river discharge. We will argue that the mechanisms presented in the 1DV framework are still present in the 2DV case.

This paper first discusses the model equations, assumptions, and the way in which the exchange flow is decomposed into different physical contributions. The contributions to the estuarine circulation are then studied in the 1DV model in section 3 by studying two cases. This allows us to develop a theoretical framework that distinguishes between two contributions to the ESCO circulation. Several important properties of these contributions will be discussed in section 4. Section 5 presents the sensitivity of the 1DV results to Simpson and unsteadiness numbers associated with well-mixed and partially stratified estuaries. The results are then generalized in a 2DV case study in section 6. Finally, we summarize and discuss our results in section 7.

2. Equations and Scaling

The exchange flow will first be studied by considering a 1DV model, since this is the simplest model that contains the interactions essential for a complete understanding of the mechanisms resulting in exchange flows. In section 6, we will generalize this to a width-averaged model example. In the 1D model, we neglect the effects of Coriolis and assume that variations of the water density are small compared to the density itself, allowing for the Boussinesq approximation. The resulting equation reads [see also *Burchard and Hetland*, 2010]

$$u_t-(A_v u_z)_z=-g[\zeta_x]-g\int_z^0 \frac{[\rho_x]}{\rho_0}d\hat{z}. \tag{1}$$

In this equation, $-H\leq z\leq 0$ is the vertical coordinate with fixed water depth H, t denotes time, u is the velocity in the along-channel direction, ρ_0 is a constant reference density of 1000 kg/m^3, g is the acceleration of gravity, and A_v denotes the eddy viscosity, which parametrizes the Reynolds stress. The model is forced by a prescribed water surface gradient $[\zeta_x]$ and density gradient $[\rho_x]$. The brackets $[\cdot]$ are used to indicate an externally prescribed forcing. The subscripts z and t in the equation denote derivatives in the vertical direction and time.

The pressure gradient $[\zeta_x]$ is chosen such that the depth-averaged velocity $\bar{u}$ satisfies

$$\bar{u}=[U]\cos(\omega t). \tag{2}$$

Here $[U]$ is a prescribed depth-averaged M_2 tidal velocity amplitude and $\omega=1.4\times10^{-4}$ s^{-1} is the angular frequency of the M_2 tide.

The boundary conditions at the free surface ($z=0$) and bed ($z=-H$) prescribe kinematic and no-slip conditions

$$A_v(0)u(0)_z=0,$$
$$u(-H)=0.$$

The turbulence closure used is the $k-\varepsilon$ model (as implemented by *Uittenbogaard et al.* [1992] and *Dijkstra et al.* [2016]). The density input into this turbulence closure is provided by a transport equation for salinity and the UNESCO equation of state [*IOC et al.*, 2010] to convert salinity to density. The transport equation for salinity reads

$$s_t-(K_v s_z)_z=-u[s_x],$$

where s is salinity and K_v is the eddy diffusivity computed as the eddy viscosity divided by a constant Prandtl-Schmidt number with value 0.7. This model is forced by a prescribed horizontal salinity gradient, directly related to the density gradient in the momentum equation via the equation of state.

2.1. Decomposition of the Equations

In order to provide insight into different contributions to the exchange flow, we will make a decomposition of the horizontal velocity u into four different contributions. To this end, we first make a careful analysis of

the role of the tidally averaged eddy viscosity and the time-varying eddy viscosity in the generation of the exchange flow. This yields a decomposition of the velocity into a component affected only by the tidally averaged eddy viscosity and one induced by the time-varying eddy viscosity. Both components can then be separated into a part forced by the barotropic pressure gradient $[\zeta_x]$ and a part forced by the density gradient $[\rho_x]$.

Such an explicit decomposition of the velocity requires the momentum equation to be linear in u. Since the eddy viscosity depends on the velocity shear, the term $(A_v u_z)_z$ is nonlinear. In order to make a decomposition, we therefore analyze the equations using two steps. In the first step, we calculate the total exchange flow and eddy viscosity using the fully nonlinear 1DV model coupled to the $k-\varepsilon$ turbulence model. In the second step, this result is further analyzed by calculating several individual contributions to the exchange flow. This is done by inserting the eddy viscosity calculated in the first step as a known input into the momentum equation. This makes the momentum equation a linear model in u, allowing for a decomposition of the exchange flow. Since the eddy viscosity is still a function of the velocity, the above steps are repeated for every new set of parameters. It is important to note that the sum of the exchange flow contributions found in the second step is identical to the total exchange flow found in the first step.

To analyze the exchange flow in the second step, we separate the eddy viscosity into a tidally averaged part $[A_v{}^0]$ and time-varying part $[A_v{}^1]$. Since we will only consider purely periodic flows, $[A_v{}^1]$ is zero when time averaged: $[A_v]=[A_v{}^0]+[A_v{}^1]$. Later, we will also consider specific harmonic components that contribute to $A_v{}^1$, such as $A_{v_{M_2}}^1$ and $A_{v_{M_4}}^1$: the M_2 and M_4 components of $A_v{}^1$. The velocity u is decomposed accordingly into a contribution u^0, which is only influenced by the tidally averaged eddy viscosity, and a contribution u^1, which contains all contributions generated by the time-varying eddy viscosity: $u=u^0+u^1$. If $[A_v{}^1]$ is zero this implies that u^1 becomes zero as well. These decompositions are substituted into equation (1), resulting in separate equations for u^0 and u^1.

All flow components that are directly forced by the prescribed M_2 depth-averaged tidal velocity $[U]$ and density gradient $[\rho_x]$ are contained in the velocity component u^0. The corresponding equation and boundary conditions are obtained by setting $[A_v{}^1]$ to zero and read

$$u_t^0-\left([A_v{}^0]u_z^0\right)_z=-g\left[\zeta_x^0\right]-g\int_z^0\frac{[\rho_x]}{\rho_0}d\hat{z},\quad\bullet\quad[A_v{}^0](0,t)u_z^0(0,t)=0,\quad\bullet\quad u^0(-H,t)=0, \tag{3}$$

where the barotropic pressure gradient $\left[\zeta_x^0\right]$ is defined such that

$$\bar{u}^0=[U]\cos(\omega t). \tag{4}$$

Equation (3) can be separated into an equation describing the velocity resulting from the barotropic tidal pressure and the velocity resulting from the baroclinic pressure (i.e., density gradient). In other words, we separate u^0 into u^{t0}, the barotropic tidal part, and u^{g0}, the baroclinic or gravitational part, such that $u^0=u^{t0}+u^{g0}$. We thus obtain (omitting the boundary conditions for brevity)

$$u_t^{t0}-\left(\left[A_v{}^0\right]u_z^{t0}\right)_z=-g\left[\zeta_x^{t0}\right], \tag{5}$$

$$-\left(\left[A_v{}^0\right]u_z^{g0}\right)_z=-g\left[\zeta_x^{g0}\right]-g\int_z^0\frac{[\rho_x]}{\rho_0}d\hat{z}. \tag{6}$$

Equation (5) defines the classical equation for the linear propagation of a tidal wave under linear friction. The forcing $\left[\zeta_x^{t0}\right]$ is such that (4) holds. Equation (6) describes the classical gravitational circulation. Hence, the time derivative and the depth average of u^{g0} are both zero. This condition defines the corresponding pressure gradient $\left[\zeta_x^{g0}\right]$.

The equation for the velocity u^1, induced by time variations of the eddy viscosity, reads

$$u_t^1-\left(\left[A_v{}^0\right]u_z^1\right)_z-\left(\left[A_v{}^1\right]u_z^1\right)_z=-g\left[\zeta_x^1\right]+\left[\left(A_v{}^1u_z^0\right)_z\right], \tag{7}$$

$$\bullet\quad[A_v{}^0(0,t)]u_z^1(0,t)+[A_v{}^1(0,t)]u_z^1(0,t)=-\left[A_v{}^1(0,t)u_z^0(0,t)\right],\quad\bullet\quad u^1(-H,t)=0. \tag{8}$$

This equation is forced by $\left[\left(A_v{}^1u_z^0\right)_z\right]$ on the right-hand side of the equation and $-\left[A_v{}^1(0,t)u_z^0(0,t)\right]$ at the right-hand side of the boundary condition. These terms describe the interaction between the time-varying

eddy viscosity and the velocity gradient of the flow affected only by the tidally averaged eddy viscosity. This forcing term is known explicitly since $A_v{}^1$ is prescribed and u^0 follows from (3). The water level gradient $\left[\zeta_x^1\right]$ is defined such that

$$\bar{u}^1 = 0.$$

This implies that u^1 only contains contributions with a depth-averaged value of zero.

The velocity u^1 is also decomposed into two contributions. We define u^{t1} as the velocity induced by interactions of $A_v{}^1$ with the barotropically forced velocity u^{t0}, i.e., $\left[\left(A_v{}^1 u_z^{t0}\right)_z\right]$. The second contribution, u^{g1}, is defined as the velocity induced by interactions of $A_v{}^1$ with the baroclinically forced velocity u^{g0}, i.e., $\left[\left(A_v{}^1 u_z^{g0}\right)_z\right]$. It holds that $u^1 = u^{t1} + u^{g1}$. We thus obtain

$$u_t^{t1} - \left(\left[A_v{}^0\right] u_z^{t1}\right)_z - \left(\left[A_v{}^1\right] u_z^{t1}\right)_z = -g\left[\zeta_x^{t1}\right] + \left[\left(A_v{}^1 u_z^{t0}\right)_z\right], \tag{9}$$

$$u_t^{g1} - \left(\left[A_v{}^0\right] u_z^{g1}\right)_z - \left(\left[A_v{}^1\right] u_z^{g1}\right)_z = -g\left[\zeta_x^{g1}\right] + \left[\left(A_v{}^1 u_z^{g0}\right)_z\right]. \tag{10}$$

The flow resulting from (9) is induced by interactions between the time variations of the eddy viscosity and the barotropic tide. Hence, the subtidal part of the solution u^{t1} will be referred to as the contribution from *tidal eddy viscosity-shear covariance (tidal ESCO or t-ESCO)*. Similarly, the flow resulting from (10) is induced by interactions between the time variations of the eddy viscosity and the classical gravitational circulation. The subtidal part of the flow u^{g1} will hence be referred to as the contribution by *gravitational eddy viscosity-shear covariance (gravitational ESCO or g-ESCO)*. Both u^{t1} and u^{g1} also contain tidally varying velocity components, but we will focus here on the subtidal components.

3. Tidal and Gravitational ESCO Circulation

Equations (9) and (10) will be used to show how the time-varying eddy viscosity contributes to the estuarine circulation. The time variations of the eddy viscosity $\left[A_v{}^1\right]$ appear both in the known forcing terms $\left[\left(A_v{}^1 u_z^{t0}\right)_z\right]$ and $\left[\left(A_v{}^1 u_z^{g0}\right)_z\right]$ on the right-hand side, as well as in the diffusive terms $\left(\left[A_v{}^1\right] u_z^{t1}\right)_z$ and $\left(\left[A_v{}^1\right] u_z^{g1}\right)_z$ on the left-hand side. All four terms containing A_{v1} contribute to the horizontal flow at multiple tidal frequency components and, depending on the frequency components of the velocity and eddy viscosity, the exchange flow. The right-hand side forcing terms can only generate an exchange flow through the interaction between a velocity shear component and eddy viscosity component on the same frequency. (Too see this, consider $\left[\left(A_v{}^1 u_z^{t0}\right)_z\right]$, where the time-varying eddy viscosity only has one constituent with angular frequency $m\omega$ and the velocity u^{t0} only has one tidal constituent with angular frequency $n\omega$. The product of both consists of two contributions with frequencies $(n+m)\omega$ and $|n-m|\omega$. Since an exchange flow by definition has an angular frequency of zero, it will only be generated if $m = n$, i.e., if the velocity and eddy viscosity components have the same frequency.) We will call such interactions *direct interactions*. The direct interactions are calculated by ignoring the left-hand side diffusion terms containing $\left[A_v{}^1\right]$. Demonstrating this using equation (6) yields

$$u_t^{t1,\mathrm{direct}} - \left(\left[A_v{}^0\right] u_z^{t1,\mathrm{direct}}\right)_z = -g\left[\zeta_x^{t1,\mathrm{direct}}\right] + \left[\left(A_v{}^1 u_z^{t0}\right)_z\right], \tag{11}$$

where $\left[\zeta_x^{t1,\mathrm{direct}}\right]$ follows from requiring $\bar{u}^{t1,\mathrm{direct}} = 0$.

The generation of exchange flows is more complex for the left-hand side diffusive terms, since they are not predetermined forcing terms, but instead depend on the solution itself. Exchange flows can therefore be generated through interactions between the velocity shear and eddy viscosity of different frequency components as well, through a set of interactions that we will explain in more detail below. We will call such interactions *indirect interactions*. The indirect interactions for the tidal ESCO follow from the difference of equations (9) and (11) and similar for the gravitational ESCO. By making a distinction between direct and indirect interactions below, we will identify new contributions to and dependencies of the exchange flow.

We will use two cases to illustrate how exchange flows are created. The typical depth, velocity, salinity gradient, and roughness used for these cases are characteristic for the Ems and the Scheldt River estuaries [see *Burchard et al.*, 2013]. The eddy viscosity is calculated using the 1DV $k-\varepsilon$ model and further analyzed using a harmonic analysis. The main time-varying eddy viscosity components are the M_2 and M_4 components, in

Table 1. Parameters Used in the Reference Cases, Corresponding to the Typical Values in the Ems and Scheldt Rivers[a]

Parameter	Symbol	Ems Case	Scheldt Case
Depth	H	7 m	8 m
Depth-averaged velocity amplitude	U	0.9 m/s	0.8 m/s
Along-channel salinity gradient	s_x	-1.0×10^{-3} psu/m	-1.5×10^{-3} psu/m
Dimensionless roughness height	z_0/H	6×10^{-5}	6×10^{-5}
Depth-averaged tidally averaged eddy viscosity	$\overline{A_v}$	8.5×10^{-3} m^2/s	2.2×10^{-2} m^2/s
Fraction M_2/tidal-mean eddy viscosity	$\lvert A_{v M_2}^1 \rvert / A_v{}^0$	0.22	0.11
Phase M_2 eddy viscosity with respect to M_2 velocity	$\phi(A_{v M_2}^1)$	45°	62°
Fraction M_4/tidal-mean eddy viscosity	$\lvert A_{v M_4}^1 \rvert / A_v{}^0$	0.84	0.70
Phase M_4 eddy viscosity with respect to M_2 velocity	$\phi(A_{v M_4}^1)$	22°	16°

[a]The eddy viscosity magnitude and phase follow from the 1DV $k-\varepsilon$ model and a harmonic analysis of the result. The other parameters are derived from *Burchard et al.* [2013].

both cases covering about 90% of the total time variation. All parameter values and a summary of the turbulence data are listed in Table 1.

3.1. Tidal ESCO Circulation

The water motion in equation (9) is forced by $\left[\left(A_v{}^1 u_z^{t0}\right)_z\right]$. This forcing term forms the basis of the original interpretation of the exchange flow due to tidal ESCO by *Jay and Musiak* [1994]. In this interpretation, the main M_2 tidal constituent (u^{t0}) and the time variable eddy viscosity at M_2 frequency ($[A_{v M_2}^1]$) interact to create an exchange flow u^{t1}. The left-hand side diffusive term $\left([A_v{}^1] u_z^{t1}\right)_z$ was not considered in their interpretation. This seems reasonable, since the generated exchange flow is typically much smaller than the M_2 tidal velocity amplitude. So although the exchange flow shear (in u_z^{t1}) could interact with the M_2 eddy viscosity in this diffusive term, this interaction is likely to be small. We call the described M_2–M_2 interaction of *Jay and Musiak* [1994] a direct interaction, as the interaction between the velocity gradient and eddy

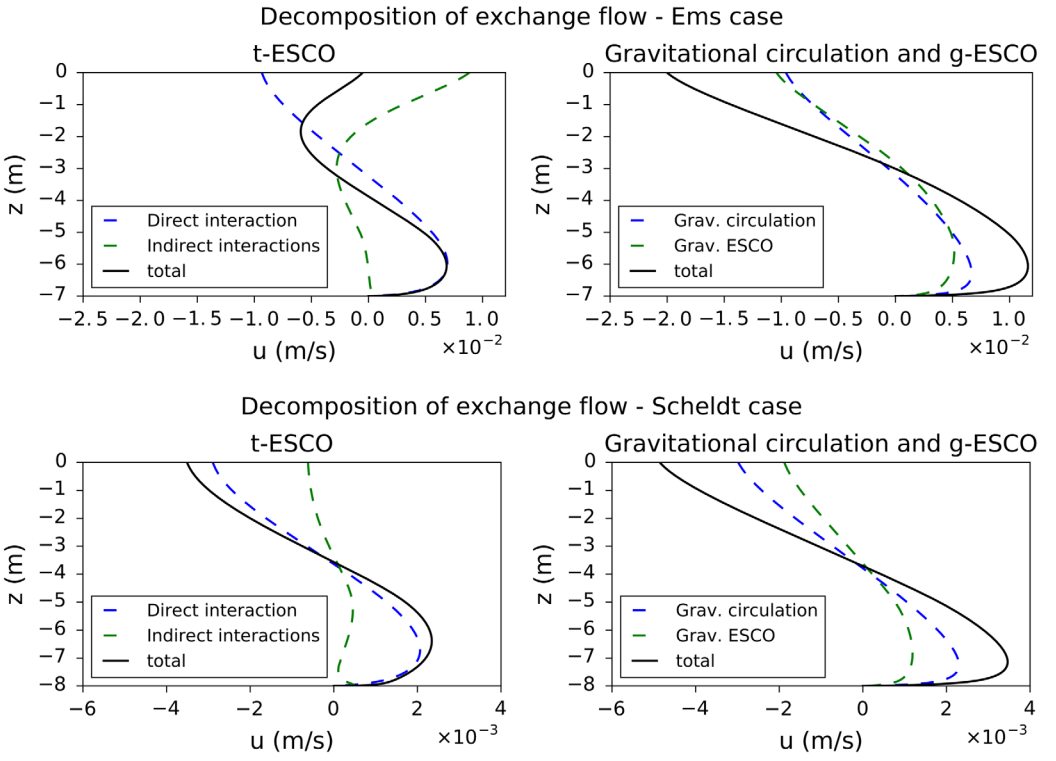

Figure 1. Vertical profiles of (left) tidal ESCO circulation and (right) gravitational circulation and gravitational ESCO in the (top) Ems River and (bottom) Scheldt River configurations (Table 1). The tidal ESCO circulation is mainly caused by the direct interaction (blue dashed line) between the tide and M_2 variations of the eddy viscosity. The remaining indirect interactions (green dashed line) between the barotropic flow and M_2 and M_4 eddy viscosity components are somewhat smaller. The gravitational circulation and gravitational ESCO circulation are of a similar order of magnitude in both cases.

viscosity immediately generate an exchange flow. This direct interaction is compared to other indirect interactions in Figure 1 (left), which show different contributions to the tidal ESCO circulation in the reference cases (Table 1). The blue lines show the exchange flow resulting from the direct M_2–M_2 interaction. While this approximates the total tidal ESCO circulation reasonably well, the exchange flow generated by indirect interactions is not negligible.

Exchange flow contributions due to indirect interactions (green lines in the left figures) are generated by many mechanisms. Each of these mechanisms individually is capable of creating an exchange flow of a similar magnitude as that generated by the direct interaction. However, different indirect interactions generate exchange flow components with opposite directions that approximately cancel against each other. The reason why individual indirect interactions can lead to a significantly large exchange flow is related to the presence of a relatively large M_4 component of the eddy viscosity. This is best understood in steps, also illustrated in Figure 2. In the left figures, the figure shows the barotropic pressure (top left) and resulting M_2 tidal flow (bottom left). This flow interacts with $A_v{}^1$ and leads to a forcing $\left[\left(A_v{}^1 u_z^{t0}\right)_z\right]$ (top middle). Through equation (11), this forcing results in the tidal ESCO circulation due to not only the direct M_2–M_2 interaction but also M_2 and M_4 flow components (bottom middle). These flow components $u_{M_2}^{t1}$ and $u_{M_4}^{t1}$ interact with the M_2 and M_4 eddy viscosity respectively in the left-hand side diffusion term (equation (9)) and lead to a forcing at several frequency components, including the subtidal component, which is displayed in Figure 2 (top right). This forcing leads to an additional contribution to the tidal ESCO circulation, as shown in the bottom right figures. This contribution has the opposite direction to a classical exchange flow. In this case, because we require two steps of interactions (or two approximations) to find an exchange flow contribution, we will call this two-step indirect interactions. The described two-step interactions, together with the direct interaction, are depicted schematically in Expressions (12)–(14).

$$\text{Direct interaction} \qquad A_{v M_2}^1 u_{z,M_2}^{t0} \rightarrow \text{exchange flow}, \tag{12}$$

$$\text{Two-step interactions} \qquad A_{v M_4}^1 u_{z,M_2}^{t0} \rightarrow u_{M_2}^{t1} \Rightarrow A_{v M_2}^1 u_{z,M_2}^{t1} \rightarrow \text{exchange flow}, \tag{13}$$

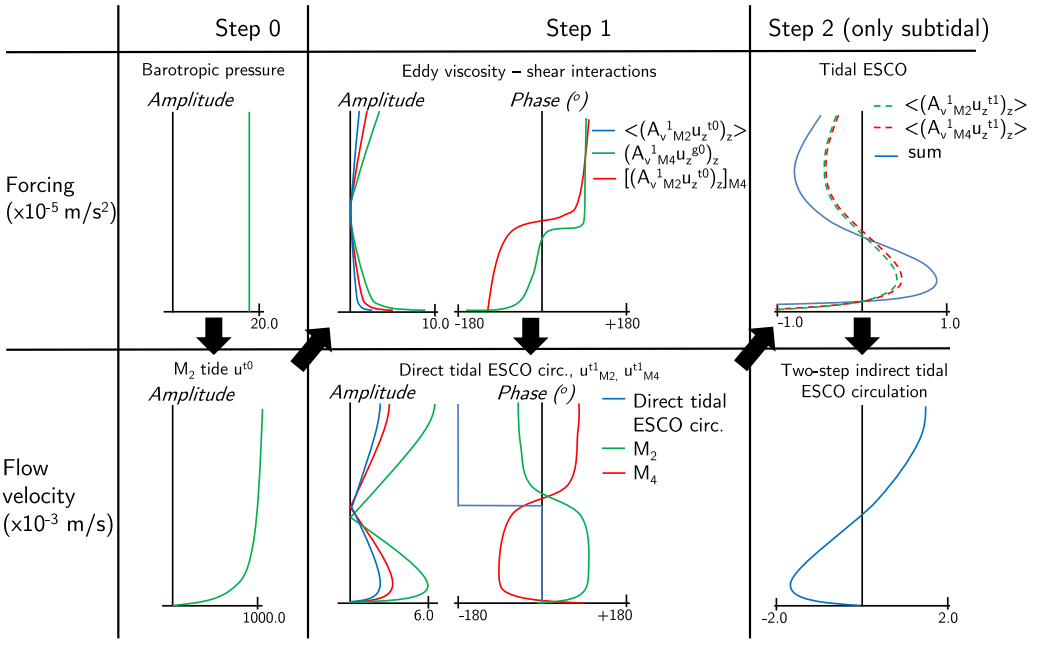

Figure 2. Sketch of the forcing terms and velocity profiles relevant to the direct and two-step indirect interactions that contribute to the tidal ESCO circulation. The shape of the profiles sketched and the order of magnitudes are derived from the results of the Scheldt case (Table 1). (left) The barotropic pressure and resulting M_2 tidal flow. (middle) How the tidal flow forces the direct tidal ESCO circulation and an M_2 and M_4 flow component through interactions with the time-varying eddy viscosity. These velocity components again interact with the time-varying eddy viscosity. This interaction lead to multiple frequency components, of which (right) shows the subtidal contribution. This forces the two-step indirect contribution to the tidal ESCO circulation. Contributions to this flow through more than two steps can be found by repeating the reasoning of this figure with more steps.

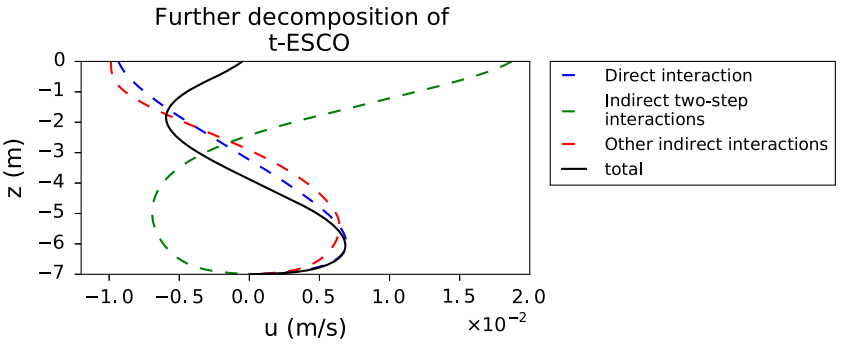

Figure 3. Further decomposition of the tidal ESCO circulation in the Ems River configuration. The exchange flow described by two interactions between the velocity and eddy viscosity is of a similar magnitude as that caused by the direct M_2–M_2 interaction but has an opposite sign. Other indirect interactions described by more interaction steps lead to an exchange flow with a positive sign. The total of all indirect interactions corresponds to the small, oddly shaped exchange flow observed in Figure 1.

$$A_{v\,M_2}^{1}\,u_{z,M_2}^{t0} \rightarrow u_{M_4}^{t1} \Rightarrow A_{v\,M_4}^{1}\,u_{z,M_4}^{t1} \rightarrow \text{exchange flow.} \tag{14}$$

Figure 3 shows a further decomposition of the indirect interactions contributing to tidal ESCO circulation by separating two-step indirect interactions in the Ems case. The total and direct contributions in this figure are identical to those shown in Figure 1. The Scheldt case gives qualitatively similar results. The exchange flow by the two-step interactions is of a similar shape and size as the exchange flow by the direct M_2–M_2 interaction but has an opposite sign. There are more indirect interactions that can only be found by making three or more steps of interactions between the velocity and time-varying eddy viscosity. These, as Figure 3 shows, result in an exchange flow in the same direction as the total tidal ESCO circulation. The combined result of the two-step and other multiple-step interactions is therefore smaller than the individual contributions to it.

The distinction between different types of indirect interactions is relevant, because the magnitude and direction of the exchange flow created by a particular set of interactions critically depends on the relative phase of all involved eddy viscosity components. As the M_2 and M_4 eddy viscosity components are typically the most dominant components, the phase difference between the M_2 and M_4 eddy viscosity and the M_2 velocity is the most important. As a result, the total exchange flow caused by indirect interactions may well be larger than that caused by direct interaction if the M_2 and M_4 eddy viscosity phases are different. We will consider this further in section 4.2.

3.2. Gravitational ESCO Circulation

Indirect interactions lead to a newly identified contribution to the exchange flow resulting from the classical gravitational circulation. This exchange flow is an amplification of the classical gravitational circulation due to interactions between the gradient of the gravitational circulation and time variations of the eddy viscosity. We will call the subtidal part of this contribution the *gravitational ESCO circulation*.

The gravitational ESCO contribution is the subtidal part of u^{g1} in (10). The generation of this term is explained using Figure 4. In the left column, the figure shows the profile of the baroclinic pressure (top left), which generates the gravitational circulation (bottom left). Considering the direct interactions and so neglecting the left-hand side term $\left[\left(A_v^{\,1}u_z^{g1}\right)_z\right]$, the gravitational circulation u^{g0} interacts with both the M_2 and M_4 eddy viscosity components in $[A_{v1}]$, leading to the forcing term in the top middle. In the Scheldt River case, this forcing has a similar amplitude as the original baroclinic pressure forcing. This generates a contribution to the M_2 and M_4 velocity: $u_{M_2}^{g1}$ and $u_{M_4}^{g1}$ (bottom middle). The M_2 and M_4 flow components have profiles that resemble an exchange flow and, in the Scheldt case, have magnitudes similar to the gravitational circulation. The phase of the forcing and flow in the middle figures depends entirely on the phase of the eddy viscosity components, but the resulting phase profile is not trivial. Next considering the indirect interactions, $u_{M_2}^{g1}$ and $u_{M_4}^{g1}$ again interact with the M_2 and M_4 eddy viscosity in the left-hand side diffusion terms (see equation (10)) resulting in a forcing term at multiple frequencies. In the top-right plot, we only show the subtidal component of this forcing, which is smaller than the baroclinic pressure forcing, but still of the same order of magnitude in the Scheldt case. This forcing leads to an exchange flow that contributes

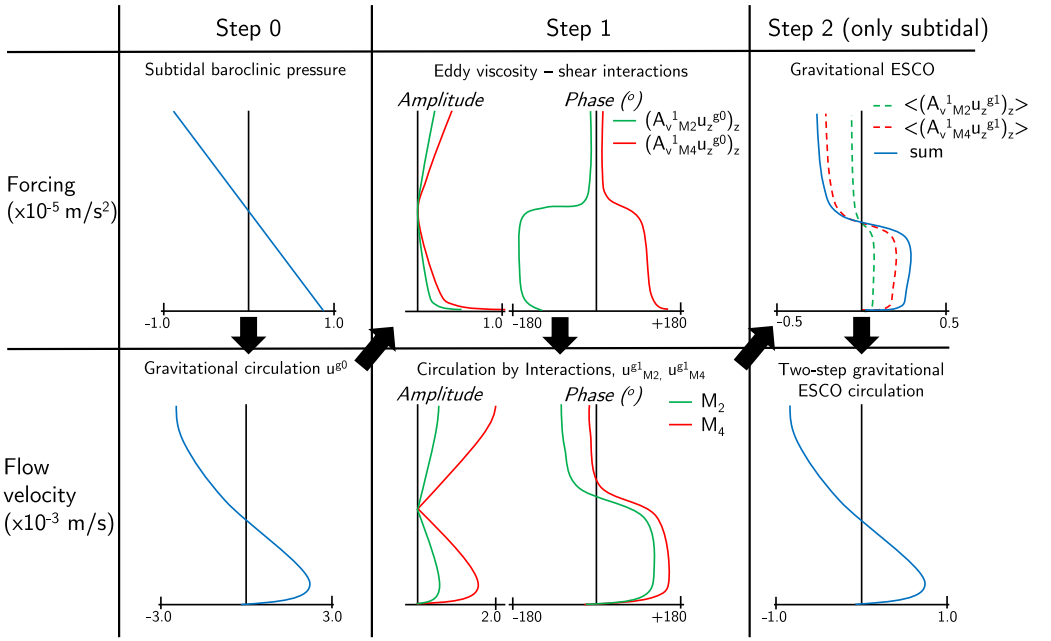

Figure 4. Sketch of the forcing terms and velocity profiles relevant to the two-step indirect interactions that contribute to the gravitational ESCO circulation. The shape of the profiles sketched and the order of magnitudes are derived from the results of the Scheldt case (Table 1). (left) The baroclinic pressure and gravitational circulation. (middle) How the gravitational circulation forces an M_2 and M_4 flow through interactions with the time-varying eddy viscosity. These velocity components again interact with the time-varying eddy viscosity. This interaction lead to multiple frequency components, of which (right) shows the subtidal contribution. This forces the two-step indirect contribution to the gravitational ESCO circulation. Contributions to this flow through more than two steps can be found by repeating the reasoning of this figure with more steps.

to the gravitational ESCO circulation and is of a similar order of magnitude and in the same direction as the gravitational circulation.

This sequence of interactions is alternatively displayed in Expressions (15) and (16). Most notably, the interaction between $u^{g1}_{M_4}$ and the relatively large M_4 eddy viscosity (equation (16)) provides a strong contribution to the exchange flow. This exchange flow contribution is found by two-step indirect interactions. Multiple-step interactions are relevant as well and will also contribute to the gravitational ESCO circulation.

$$\text{Two-step indirect interactions} \qquad A^1_{\nu M_2} u^{g0}_z \rightarrow u^{g1}_{M_2} \Rightarrow A^1_{\nu M_2} u^{g1}_{z,M_2} \rightarrow \text{exchange flow}, \tag{15}$$

$$A^1_{\nu M_4} u^{g0}_z \rightarrow u^{g1}_{M_4} \Rightarrow A^1_{\nu M_4} u^{g1}_{z,M_4} \rightarrow \text{exchange flow}. \tag{16}$$

Figure 1 (right) shows the resulting magnitudes of the gravitational ESCO circulation compared to the gravitational circulation in the Ems and Scheldt River cases (Table 1). The figures show that the gravitational ESCO circulation is of a similar magnitude as the classical gravitational circulation in the Ems case and about half the size of the gravitational circulation in the Scheldt case. The difference between the cases follows from the observation that M_2 and M_4 eddy viscosity amplitudes are smaller in the Scheldt River case than those in the Ems River case.

4. Dependencies of Tidal and Gravitational ESCO Circulation

In this section, we will study the sensitivity of the tidal and gravitational circulation to the amplitude (section 4.1) and phase (section 4.2) of the temporally varying eddy viscosity. The default parameter settings for this sensitivity study are for the Scheldt River case, as shown in Table 1. The M_2 component of the eddy viscosity calculated for this case is multiplied by a factor to change the amplitude (section 4.1) or phase (section 4.2). Physically, this could roughly represent a change to the M_2 eddy viscosity component by processes not accounted for in the 1-D model. The newly obtained eddy viscosity field is used to recalculate and decompose the exchange flow.

The results will be analyzed using a measure for the magnitude of the exchange flow according to

$$\mathcal{M}(u)=\sigma\frac{1}{H}\int_{-H}^{0}|u(z)-\bar{u}|\,dz, \tag{17}$$

where $\bar{u}$ denotes the depth average and

$$\sigma=\text{sign}\left(\frac{2}{H}\int_{-H}^{-H/2}u(z)-\bar{u}\,dz\right).$$

We thus take the integral of the absolute value of the tidally averaged flow, minus any depth-averaged tidally averaged contribution, such as the river discharge. While this is not relevant in our 1DV model, the 2DV model discussed later does allow for river discharge. The parameter σ adds a sign to the exchange flow, stating it is positive when the flow is upstream in the lower half of the water column. As a consequence, the classical gravitational circulation in an estuary is considered positive.

4.1. Dependence on the Eddy Viscosity Amplitude

Figure 5 shows the dependence of the tidal and gravitational ESCO circulation to variations of the M_2 eddy viscosity amplitude. The M_2 eddy viscosity amplitude $|A_{v\,M_2}^{1}|$ is varied between 0 and 20% of the tidal-mean eddy viscosity $A_{v\,M_0}^{0}$, which is not varied. A larger amplitude of the M_2 eddy viscosity could not be tested, as this would cause the eddy viscosity to become negative. The other parameters have their default values.

The figure shows that the tidal ESCO circulation vanishes for vanishing M_2 eddy viscosity. This is because all interactions leading to tidal ESCO circulation with the M_2 tide involve the M_2 eddy viscosity, see also (12)–(14). The direct M_2–M_2 contribution to the tidal ESCO circulation (dashed line) scales linearly with the M_2 eddy viscosity amplitude. This is because its forcing term $\left[\left(A_v^{\,1}u_z^{t0}\right)_z\right]$ scales linearly with the M_2 eddy viscosity in $[A_v^{\,1}]$. The two-step interactions depend linearly on the M_2 eddy viscosity, but interactions involving more steps may also depend on higher odd powers of the M_2 eddy viscosity. This is why the total effect of indirect interactions (difference between solid line and dashed line) increases nonlinearly with the M_2 eddy viscosity amplitude.

The gravitational ESCO circulation is nonzero for vanishing M_2 eddy viscosity. Even if the M_2 eddy viscosity is zero, indirect interactions with other time-varying eddy viscosity components, here the M_4 component, still contribute to the gravitational ESCO circulation. The main contribution to the gravitational ESCO circulation involving the M_2 eddy viscosity is the two-step interaction of Expression (15). This involves the M_2 eddy viscosity in two steps and thus leads to an approximately quadratic dependence of the gravitational ESCO circulation on the M_2 eddy viscosity amplitude.

4.2. Dependence on the Eddy Viscosity Phase

Figure 6 shows how the tidal and gravitational ESCO circulation depend on the phase of the M_2 eddy viscosity ϕ_{M_2}, which is defined as the phase relative to the depth-averaged M_2 tidal velocity. The phase ϕ_{M_2} is varied between 0° and 360°. The magnitude of the tidal ESCO circulation varies strongly with the M_2 eddy

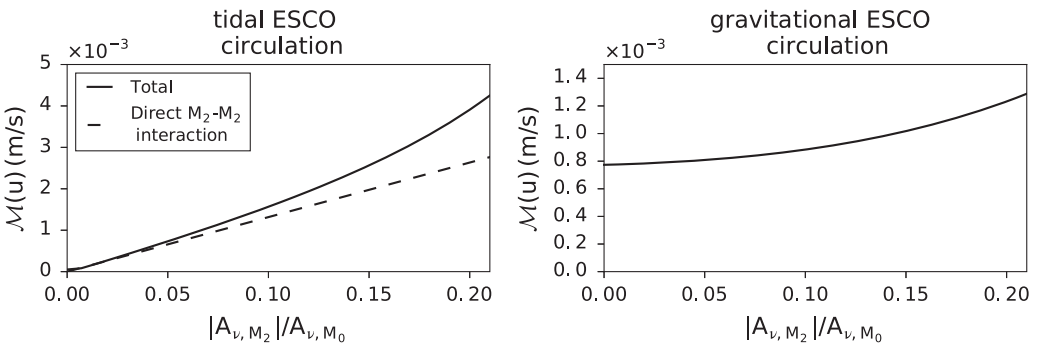

Figure 5. Dependence of the tidal and gravitational ESCO circulation magnitude $\mathcal{M}(u)$ on the amplitude of the M_2 eddy viscosity component in the Scheldt configuration (Table 1). The tidal ESCO circulation is zero for vanishing M_2 eddy viscosity and then shows an almost linear dependence for $|A_{v\,M_2}|/A_{v\,M_0}$ up to 10–15%. It can be well approximated by the linear dependence of the direct M_2–M_2 interactions. The gravitational ESCO circulation is nonzero for vanishing M_2 eddy viscosity due to remaining interactions with the M_4 eddy viscosity. It has an approximate quadratic dependence on $|A_{v\,M_2}|/A_{v\,M_0}$.

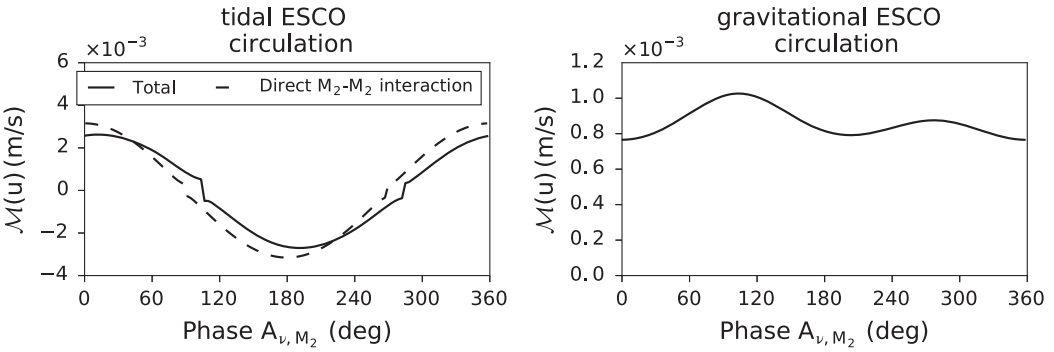

Figure 6. Dependence of the tidal and gravitational ESCO circulation magnitude $\mathcal{M}(u)$ on the phase difference between the M_2 eddy viscosity and the M_2 tidal velocity. The results are for the Scheldt River case (Table 1). The tidal ESCO circulation shows a strong dependency and almost vanishes for a 100° and 190° phase difference. The gravitational ESCO circulation shows a weaker dependency, because it is largely caused by phase-independent interactions.

viscosity phase. It attains its maximum for phases of 10° and 190° and almost vanishes for phases of 100° and 280°. Most of this behavior can be explained using the direct M_2–M_2 interaction (dashed line). This interaction depends linearly on the M_2 eddy viscosity, resulting in a strength of the tidal ESCO circulation that is proportional to the cosine of ϕ_{M_2}.

The total tidal ESCO circulation can be either larger or smaller than the exchange flow by the direct interaction due to the effect of indirect interactions. As already noted in section 3, the magnitude and direction of the exchange flow caused by indirect interactions depends strongly on the phase difference between the M_2 and M_4 eddy viscosity components. While keeping the phase of the M_4 eddy viscosity constant, we see a complex dependence of the indirect interaction on the M_2 eddy viscosity phase. Indirect interactions decrease the total exchange flow between $\phi_{M_2}=50°$ and 230° and increase it otherwise. The sudden jumps around the zero-crossings are an artifact resulting from our choice to keep the vertical distribution of the phase difference constant throughout the experiment, which is not entirely realistic. A smooth transition is expected when allowing for the phase of the M_2 eddy viscosity to vary over the water column as well.

The magnitude of the gravitational ESCO circulation is less sensitive to the phase of the M_2 eddy viscosity. The direction of the exchange flow furthermore remains positive, independent of the relative phase of the eddy viscosity. The magnitude is largest for an M_2 eddy viscosity phase of 90° and 270° and reaches a minimum for a phase of 0° and 180°. To elucidate this behavior, consider a case with only an M_2 eddy viscosity component. The interaction between the gravitational circulation and M_2 eddy viscosity results in a contribution to the M_2 velocity, which is approximately in phase with the M_2 eddy viscosity. This M_2 velocity contribution interacts with the M_2 eddy viscosity again to create an exchange flow. The M_2 velocity contribution and eddy viscosity always have the same small phase difference, regardless of the phase of the M_2 eddy viscosity. So their interaction always leads to the same exchange flow, regardless of the phase of the M_2 eddy viscosity. The variations in the magnitude of the exchange flow are a consequence of three-step or higher interactions, which use a combination of the M_2 and M_4 eddy viscosity components and therefore depend on their relative phase difference. The phase difference between these two eddy viscosity components changes when the phase of the M_2 eddy viscosity is changed, thus affecting the resulting magnitude of the exchange flow.

5. Parameter Space Dependency of the Exchange Flow

It has been shown by *Baumert and Radach* [1992] and *Burchard* [2009] that the parameter sensitivity in a 1DV model without Coriolis can be captured in three dimensionless parameters: the inverse Stokes number or unsteadiness number Un [*Burchard et al.*, 2011], the Simpson number Si, and the dimensionless roughness height z_0^*:

$$\mathrm{Un}=\frac{\omega H}{u_*},\quad \mathrm{Si}=\frac{b_x H^2}{u_*^2},\quad z_0^*=\frac{z_0}{H}.$$

It should be noted that different authors use slightly different dimensionless parameters, e.g., by making time dimensionless using the tidal period T instead of the angular frequency ω or by making the velocity

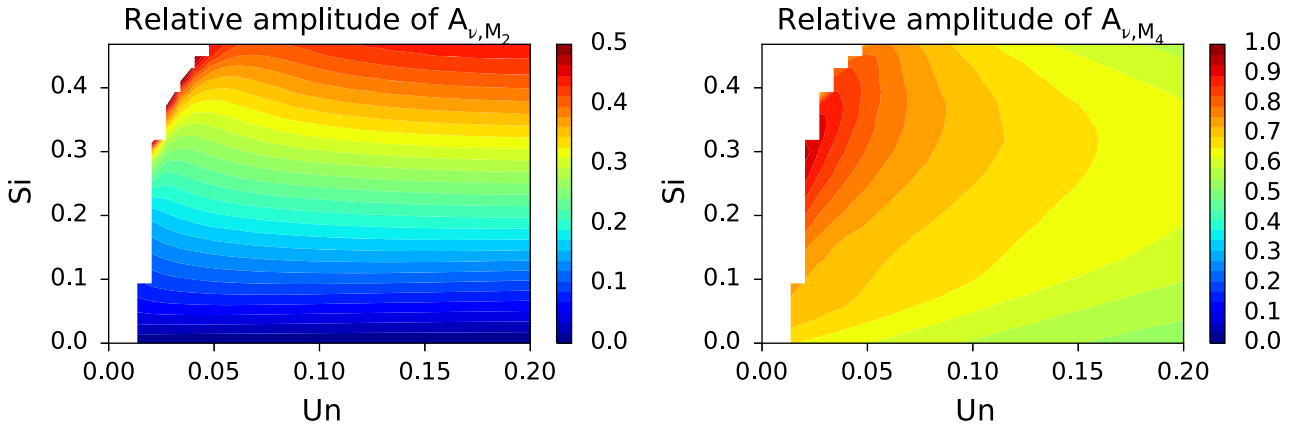

Figure 7. Sensitivity of the M_2 and M_4 eddy viscosity amplitude relative to the tidally averaged eddy viscosity to Un and Si in the 1DV model. The M_2 eddy viscosity scales dominantly with the Simpson number. The M_4 viscosity shows a variation with both the Simpson and unsteadiness numbers.

dimensionless by using the depth-averaged amplitude U instead of a typical friction velocity scale u_*. The definitions used here match those used by *Burchard et al.* [2011].

We vary the unsteadiness number between 0 and 0.2 with increments of approximately 0.007 by varying the velocity $[U]$ and the Simpson number between 0 and 0.5 with increments of 0.02 by varying the density

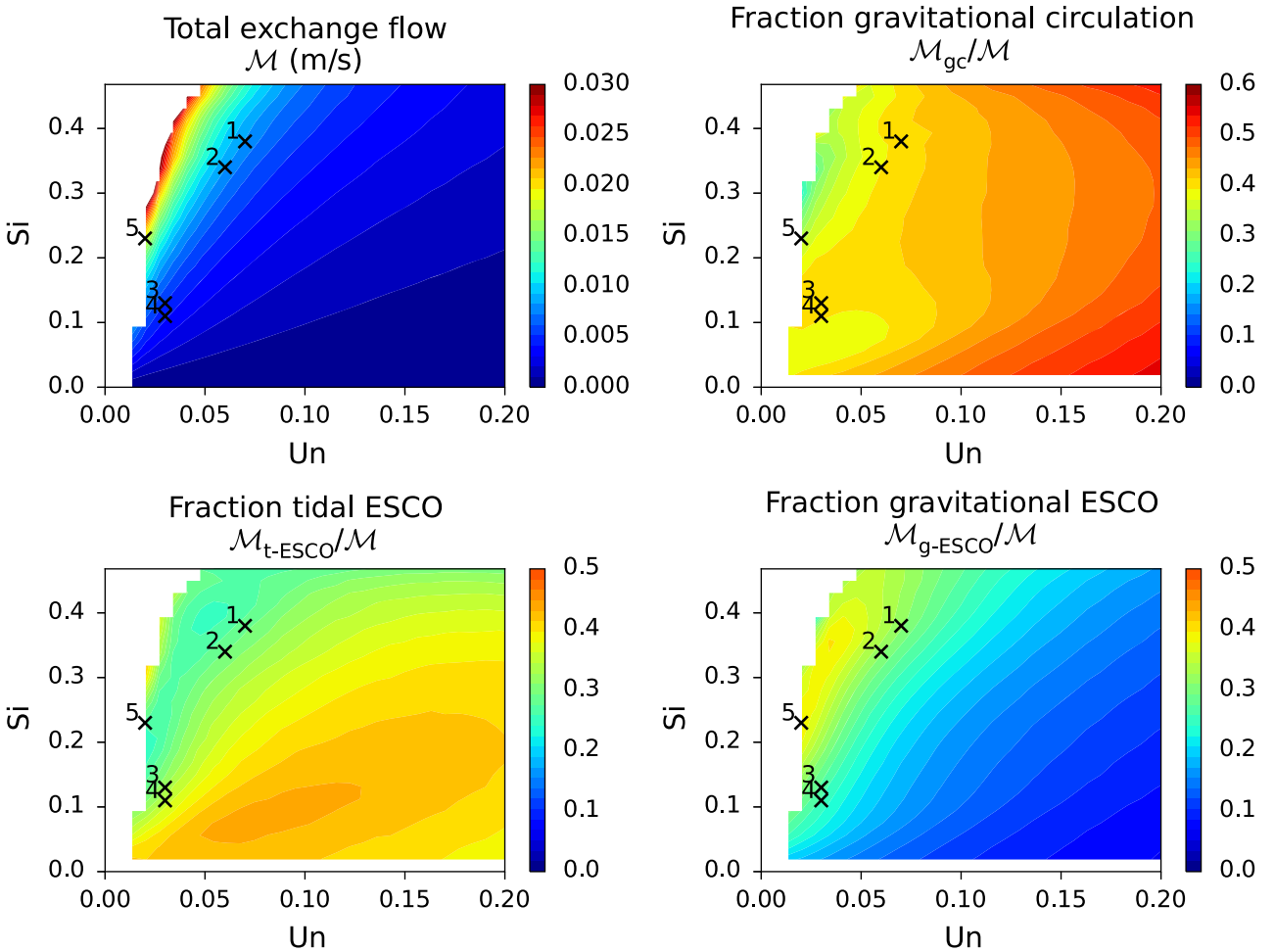

Figure 8. Sensitivity of the exchange flow magnitude to the unsteadiness number (horizontal axis) and Simpson number (vertical axis). (a) The absolute exchange flow magnitude of all mechanisms combined. (b–d) The relative contributions to this exchange flow by the gravitational circulation, tidal ESCO circulation, and gravitational ESCO circulation. The blanked out area corresponds to the area where the 1DV model assumptions are violated. The numbered crosses correspond to the estuaries listed in Table 2.

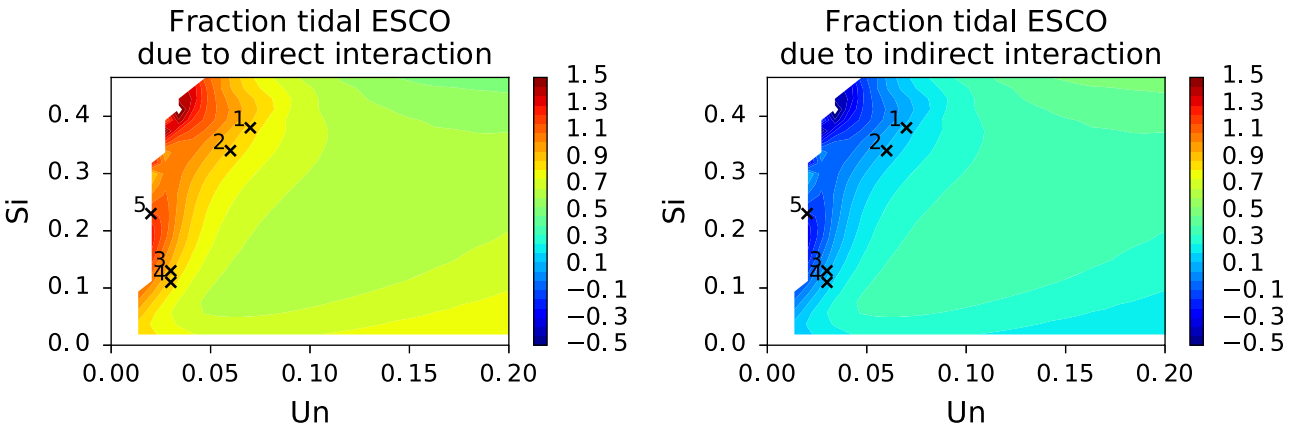

Figure 9. Magnitude of the tidal ESCO circulation contributions caused (a) by the direct M_2–M_2 interaction and (b) by indirect interactions. The given magnitudes are relative to the total tidal ESCO circulation. A negative magnitude indicates an exchange flow in the opposite direction.

gradient $[\rho_x]$. This range is similar to that used by *Burchard and Hetland* [2010]. A fixed value of the dimensionless roughness height $z_0^*=6\times10^{-5}$ is used throughout the simulation. This parameter is not varied, as the relative importance of the different exchange flow contributions is not very sensitive to it. The Simpson number has a critical maximum value in 1DV models. Above this value, the assumption of horizontal homogeneity is violated, resulting in a boundless increase in stratification [e.g., *Simpson et al.*, 1990; *Monismith et al.*, 2002; *Geyer and MacCready*, 2014]. The cases for which this happens are blanked out in Figures 7–9.

The experiments are performed using the 1DV model with $k-\varepsilon$ turbulence closure. This model uses 50 equidistant grid cells and a time step of 20 s. Each run allows for four tidal cycles of spin-up time, after which the results are a purely periodic signal.

5.1. Sensitivity to Un and Si

As the M_2 and M_4 eddy viscosity components are the most important generators of the tidal and gravitational ESCO circulation, we will first investigate the sensitivity of these components to Un and Si, see Figure 7. The M_2 eddy viscosity is mainly generated by SIPS. As explained in the introduction, SIPS typically reduces the eddy viscosity through stable stratification during ebb and increases the eddy viscosity through mixing of the stratification during flood. The strength of SIPS primarily depends on the Simpson number through a linear relation. Correspondingly, the figure shows that the M_2 eddy viscosity, relative to the tidal-mean eddy viscosity, is almost independent of the unsteadiness number and scales approximately linearly with the Simpson number $\sim$Si$^{0.9}$. The phase of the M_2 eddy viscosity (not shown) depends on timing of the stratification and destratification of the water column. This phase decreases somewhat with Un and hardly varies with Si. It is hypothesized that this is because the timing of stratification depends mainly on the mean rate of mixing of the water column, which is mainly determined by the tidal velocity, versus the tidal period. Both are associated with the barotropic tide and therefore with Un. The M_4 eddy viscosity in mainly generated by the absolute value of the tidal velocity, so that the eddy viscosity is smallest around the slack tides and largest around the peak tides. The M_4 eddy viscosity amplitude and phase (the latter not shown) are therefore mainly related to the unsteadiness number. The Simpson number has some effect on the M_4 eddy viscosity amplitude. However, this dependency is weaker and has multiple causes. These causes include the effect that stratification has on the tide and mean eddy viscosity, therefore affecting the generation of the M_4 eddy viscosity, and the direct generation of an M_4 eddy viscosity component by the stratification through nonlinear interactions in the turbulence model. No simple expression in terms of powers of Un and Si can be found for the M_4 eddy viscosity.

Figure 8a presents the absolute magnitude of the exchange flow $\mathcal{M}$ in the parameter space of unsteadiness and Simpson numbers. The total exchange flow increases for increasing Si and decreasing Un. An increasing Simpson number means an increasing influence of buoyancy, leading to a larger gravitational circulation. It also leads to a larger M_2 eddy viscosity component and therefore larger ESCO circulation. A decreasing unsteadiness number is equivalent to an increasing tidal velocity at the same depth. The exchange flow magnitude increases with the tidal velocity, because the tidal velocity gradient is the forcing for the tidal

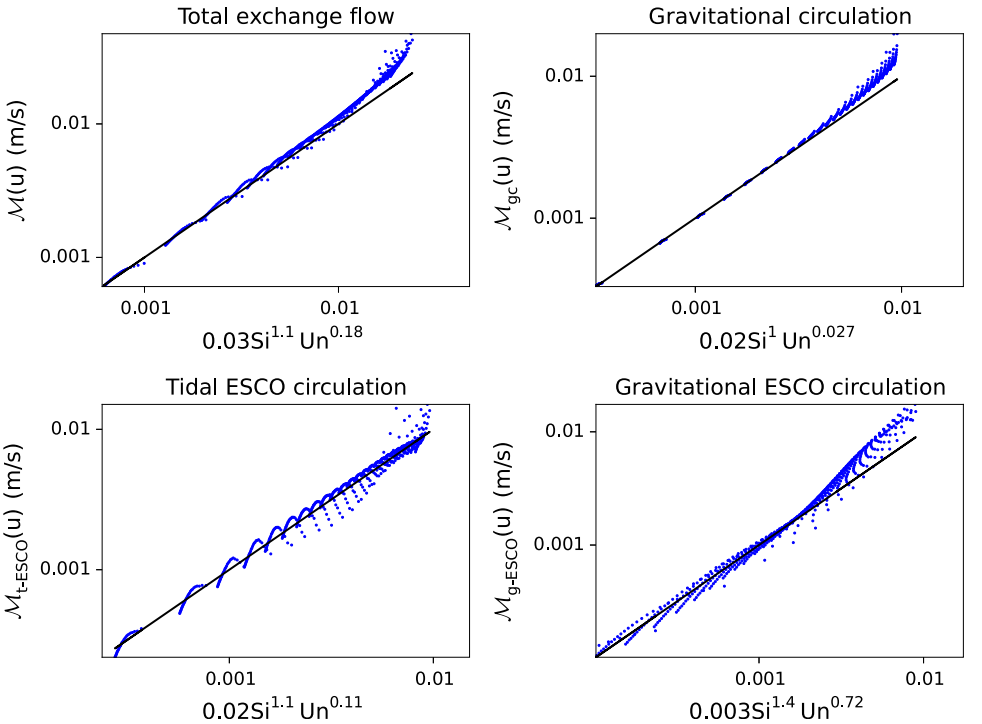

Figure 10. Fitted relations for the exchange flow magnitude and its separate contributions as a function of Si and Un. The fitting procedure uses a least squares procedure and has been set to fit closest to the lower range of values. The obtained relations for each contribution are plotted below the figures.

ESCO circulation. A decreasing unsteadiness number also leads to a larger M_4 eddy viscosity and therefore a larger ESCO circulation. We can look closer at the magnitude of the individual contributions to the total exchange flow by defining the magnitude of the gravitational circulation $\mathcal{M}_{gc}$, tidal ESCO $\mathcal{M}_{t-ESCO}$ and gravitational ESCO $\mathcal{M}_{g-ESCO}$ similar to equation (17), but then for these individual flow components.

The relative contribution of the gravitational circulation to the total exchange flow ($\mathcal{M}_{gc}/\mathcal{M}$) is 30%–50% (Figure 8b). This percentage depends only weakly on Si, which implies that its *relative* contribution is insensitive to the horizontal salinity gradient. This is because both the gravitational circulation and total exchange scale approximately linearly with the horizontal salinity gradient (see also later in Figure 10). The relative contribution of gravitational circulation increases with increasing unsteadiness number.

The tidal and gravitational ESCO circulations are responsible for the remaining 50%–70% of the exchange flow (Figures 8c and 8d). The tidal ESCO circulation is much more important than the gravitational ESCO circulation for high unsteadiness numbers and low Simpson numbers. In this range, the gravitational circulation and the M_2 (weak SIPS) and M_4 (weak friction) eddy viscosity components are relatively small. As the gravitational ESCO circulation depends on the gravitational circulation and depends approximately quadratically on the time-varying components of the eddy viscosity (see also section 4.1), its magnitude is small in this parameter range. The tidal ESCO circulation only depends linearly on the time-varying components of the eddy viscosity and is therefore relatively large compared to the gravitational ESCO circulation.

On the other hand, the gravitational ESCO circulation makes a relative contribution of 40% to the exchange flow, versus 25% by the tidal ESCO circulation, in the range of high Simpson numbers and low unsteadiness numbers. In this range, the magnitude of the gravitational circulation is relatively larger compared to the tidal velocity amplitude and the time variations of the eddy viscosity are at their maximum. These conditions favor the primarily quadratic dependence of the gravitational ESCO on the time-varying eddy viscosity.

Figure 9 shows a further decomposition of the tidal ESCO circulation into the contribution due to the direct M_2–M_2 interaction and that due to indirect interactions. The direct interaction is always the most important term. Nevertheless, the indirect interactions make a significant positive contribution to the exchange flow

Table 2. Typical Depth, Tidal Velocity, and Salinity Gradient of Five Estuaries or Tidal Inlets[a]

No.	Name of Estuary	H (m)	U_{M_2} (m/s)	s_x ($\times 10^{-4}$ psu/m)	Si	Un
1	Wadden Sea (List Deep)	14.8	0.7	1.8	0.38	0.07
2	Wadden Sea (Marsdiep Inlet)	22	1.4	2.6	0.34	0.06
3	York River (spring tide)	7	0.65	3	0.13	0.03
4	Western Scheldt River	8	0.8	2.7	0.11	0.03
5	Ems River	7	0.9	10	0.23	0.02

[a]The Simpson number Si and unsteadiness number Un have been calculated accordingly. This table is adapted from *Burchard et al.* [2013].

in the range of intermediate to large Simpson numbers and small unsteadiness numbers. Conversely, the indirect interactions make a significant contribution to reduce the exchange flow in the range of small unsteadiness numbers and large Simpson numbers.

The dimensionless parameters for a number of estuaries and tidal inlets have been indicated in Figures 8 and 9. The numbers next to the markers correspond to the numbers in Table 2, which is adapted from *Burchard et al.* [2013]. These numbers are representative for the estuaries under consideration. Note however that there is strong variation in these numbers depending on the position along the estuary (see section 6), the phase of the spring-neap cycle and the freshwater discharge. The numbers listed are thus mainly indicative. Additionally, these numbers are projected onto one-dimensional results which do not include all the possible physical mechanisms present in a three-dimensional system. Nevertheless, all the estuaries and inlets listed here are located within the range where the gravitational ESCO circulation is of the same magnitude or larger than the tidal ESCO circulation. Following the strong indications that tidal ESCO is important in many systems [e.g., see *Geyer and MacCready*, 2014, and references therein] this seems to indicate that the newly identified gravitational ESCO circulation is an important exchange flow contribution in real-world systems.

5.2. Scaling of the Exchange Flow With Un and Si

The dependence to Un and Si of the gravitational circulation and tidal and gravitational ESCO circulation to the exchange flow can be reasonably well described by a power relation of the form $\alpha \mathrm{Si}^{\beta}\mathrm{Un}^{\gamma}$. The results obtained from fitting this relation to the computed data are plotted in Figure 10. The fit is made on the basis of the smaller exchange flow magnitudes, hence the fitted line deviates from the data points for larger values. The results show that the magnitude of the gravitational circulation scales linearly with the Simpson number, consistent with the findings of *Burchard and Hetland* [2010] and the analytical expression of *Hansen and Rattray* [1965]. However, for somewhat larger values of the gravitational circulation, the scaling gradually changes to $\mathrm{Si}^{1.5}$ or more. This is caused by the stratification that starts to reduce the tidal-mean eddy viscosity as the Si number increases. As was shown by the analytical solution of *Hansen and Rattray* [1965], such a reduction of the tidal-mean eddy viscosity increases the magnitude of the gravitational circulation.

The tidal ESCO circulation also scales approximately linearly with Si and shows little deviation from this linear dependency for larger values. We have established that the M_2 eddy viscosity also scales approximately linearly with the Simpson number, so the scaling represents a linear dependency between the tidal ESCO circulation and the M_2 eddy viscosity. This is consistent with the observation that the tidal ESCO circulation consists mainly of the contribution by the direct M_2–M_2 interaction, which scales linearly with the M_2 eddy viscosity (see section 4.1).

The gravitational ESCO circulation scales with $\mathrm{Si}^{1.4}$ for small Si values and with Si^{2} for larger values. The nonlinear dependence on Si results from its nonlinear dependence on the M_2 and M_4 eddy viscosity components, which both depend on Si. The nonlinear dependence of the gravitational circulation on Si at large values additionally results in a nonlinear dependence of the gravitational ESCO circulation on Si at large values. The gravitational ESCO circulation additionally depends on a power -0.7 of the unsteadiness number. This is mainly caused by its dependence on the M_4 eddy viscosity component, which varies with Un.

The sum of the three contributions to the exchange flow results in a total flow that scales almost linearly with the Simpson number for small values of this parameter, but scales with $\mathrm{Si}^{1.5}$ for larger values. This means that the exchange flow, and in particular the contribution by the gravitational ESCO circulation,

Table 3. Parameter Values Used in the 2DV Case

Parameter	Value
Length (km)	160
M_2 tidal amplitude at mouth (m)	1.78
M_4 tidal amplitude at mouth (m)	0.13
Phase of M_4 tide relative to M_2 tide (°)	−1
River discharge (m^3/s)	20
z_0 (m)	0.005
Number of equidistant computational cells in x-direction	100
Number of equidistant computational cells in z-direction	50
Time step (only in Delft 3D) (s)	60

grows at an accelerating pace when the flow approaches the transition to a strongly stratified water column.

6. Generalization: A 2DV Test Case

In this section, we will decompose the exchange flows found using a width-averaged (2DV) shallow water model using the theoretical framework developed for the 1-D model. Whereas the exchange flow in the 1-D model only results from a linear barotropic and baroclinic pressure, the exchange flow in the width-averaged model additionally results from river induced velocity gradients and nonlinear terms, such as momentum advection and elevations of the water surface. The 2DV model is forced by an M_2 and M_4 tide at the seaward boundary and constant river discharge at the landward boundary.

In order to decompose the exchange flow, we take a similar approach as taken by *Cheng et al*. [2011, 2013] and in section 2. We use the state of the art simulation model Delft 3-D [*Deltares*, 2014] with $k-\varepsilon$ turbulence closure to compute the eddy viscosity and salinity fields. Unlike the 1DV model, the 2DV model does not reduce to a linear model when the eddy viscosity and salinity are prescribed. Therefore, the 2DV model equations are solved using a perturbation approach [*Chernetsky et al*., 2010; *Cheng et al*., 2010; *Wei et al*., 2016], where the computed eddy viscosity and salinity are used as input. These models use the assumption that the water surface elevation is small compared to the water depth, resulting in an asymptotic analysis that allows for a decomposition of the flow induced by different physical mechanisms. Here we extend this approach to allow for a no-slip boundary condition and arbitrary vertical eddy viscosity profiles and time variations of the eddy viscosity at leading order. A detailed description of this model, called *iFlow*, can be found in *Dijkstra et al.* [2017]. The perturbation model uses a fixed surface level instead of a temporally varying one. The eddy viscosity and salinity from the complex model therefore need to be interpolated and extrapolated to the fixed surface level. This interpolation and the approximations of the nonlinear terms in the perturbation model lead to differences between the results of this model and the Delft 3-D modeling suite. The perturbation model nevertheless results in a good approximation and provides a clear indication of the importance of the various exchange flow contributions.

We will investigate the relative importance of the various exchange flow contributions in the Scheldt River, using the model setup by *Brouwer et al*. [2015]. This model approximates the observed depth using a smooth function that varies between 14.5 m at the mouth and 3 m at 160 km from the mouth, where a lock complex marks the end of the tidal influence. The width varies between 6.5 km at the mouth and 40 m as the landward end. The salinity is calibrated such that the tidally averaged salinity corresponds to the multi-year average summer, i.e., low discharge, salinity profile. Details of the parameters values used are listed in Table 3.

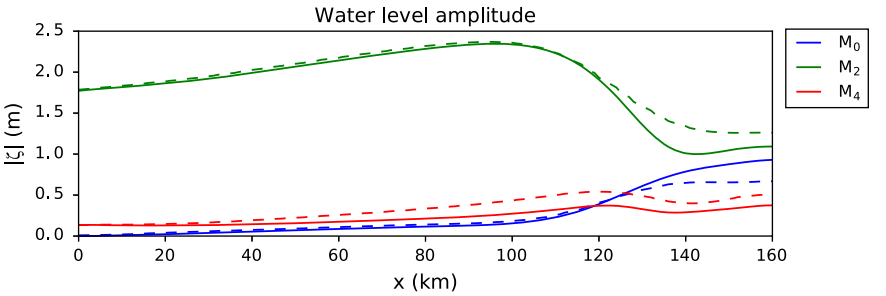

Figure 11. Water level amplitudes of the tidally averaged, M_2 and M_4 components in the 2DV case. The result of the iFlow model (solid lines) is corresponds reasonably well to the result of the Delft 3-D model (dashed lines) up to 100 km. The largest differences are found in the M_4 water level amplitude, which is underestimated in the iFlow model.

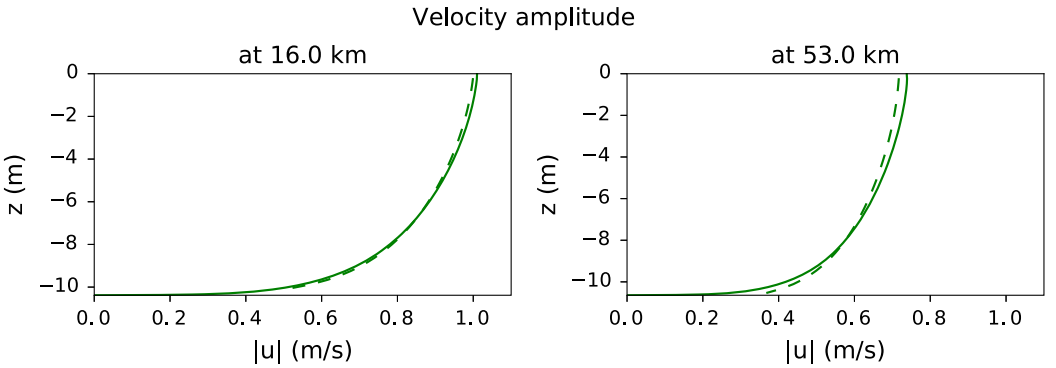

Figure 12. Comparison of the velocity amplitude profiles at 16 and 56 km from the mouth in the 2DV case with the iFlow model (solid lines) and the Delft 3-D model (dashed lines).

Figure 11 shows the tidally averaged, M_2 and M_4 surface elevation. The dashed lines show the results of the Delft 3-D model, while the solid line shows the results obtained with the perturbation model. There is a good correspondence between the results of both models up to about 100 km inland. Beyond this point, the tidal elevation is no longer small compared to the depth of the shallow river and the differences between the models are no longer negligible. The M_2 velocity profiles at two locations in both models are shown in Figure 12. There is a good correspondence between the profiles. The deviations are mainly due to the conversion of the Delft 3-D profiles from a moving reference level to fixed coordinates. Profiles of the tidally averaged and M_4 velocity cannot be compared between the models, because these components have a different interpretation in surface-following coordinates than in a fixed reference frame.

We find a number of contributions to the ESCO circulation additional to those present in the 1-D model. These include the circulation due to interactions between the time-varying eddy viscosity and the external M_4 tide, river flow, tidal return flow, and flow generated by momentum advection. The latter is named *advective ESCO circulation*. The decomposition of the exchange flow at four selected locations is presented in Table 4. The table shows the total exchange flow magnitude $\mathcal{M}(u)$ (see (17)) and the fractional contributions to this exchange flow. The table also presents the depth-averaged amplitudes of the M_2 and M_4 eddy viscosity relative to the tidally averaged eddy viscosity and the phase relative to the M_2 tidal velocity phase. Below, we will discuss the various exchange flow contributions listed in this table.

First considering the eddy viscosity, we see that the M_2 eddy viscosity amplitude is considerably larger than in the 1DV Scheldt case, where it was 11% (Table 1). At the 56 km point, this is partly because the along-

Table 4. Exchange Flow and an Approximate Decomposition Into the Relative Contributions for the 2DV Case[a]

	At 5 km	At 16 km	At 56 km	At 100 km
Total exchange flow (m/s)	0.006	0.004	0.01	0.01
Tidal ESCO circulation: M_2 tide (%)	41	47	35	12
Of which direct M_2–M_2 interactions (%)	*37*	*57*	*71*	*117*
Of which indirect interactions (%)	*63*	*43*	*29*	*−17*
Tidal ESCO circulation: M_4 tide (%)	−8	−7	−8	−1
Gravitational circulation (%)	26	19	43	1
Gravitational ESCO circulation (%)	25	9	24	0
Advection circulation (%)	8	1	−1	1
Advective ESCO circulation (%)	0	1	−1	0
Other (%)	8	30	8	87
$\lvert A_{\nu M_2}\rvert/A_{\nu M_0}$ (%)	32	27	42	35
$\lvert A_{\nu M_4}\rvert/A_{\nu M_0}$ (%)	60	54	47	29
Phase $A_{\nu M_2}$ relative to M_2 velocity (°)	88	80	65	62
Phase $A_{\nu M_4}$ relative to M_2 velocity (°)	5	2	10	17
Subtidal salinity gradient s_x ($\times 10^{-4}$ psu/m)	−1.6	−1.5	−5.1	−0.7

[a]Additionally, the relative magnitudes and phases of the M_2 and M_4 eddy viscosity and the magnitude of the horizontal salinity gradient are shown. The results are presented at four stations along estuary, the first three are in the saltwater region, while the last station is just in the freshwater area. The exchange flow contribution "other" contains the shear of the velocity profiles of the tidal return flow and river flow. Italics signifies that this is a percentage of the above percentage.

channel salinity gradient is about four times larger than in the 1DV case, leading to more SIPS and thus a larger M_2 eddy viscosity. However, the along-channel salinity gradient at 5 and 16 km is very close to the value used in the 1DV study and the salinity gradient is two times smaller at 100 km. This indicates that the M_2 eddy viscosity is affected by other mechanisms than SIPS. Besides SIPS, the two most dominant mechanisms are the M_2 variation of the water depth and tidal velocity asymmetry.

At all locations except for 56 km, it is found that the tidal ESCO circulation by the M_2 tide is, in a relative sense, larger compared to the gravitational circulation and gravitational ESCO circulation than in the 1-D model. This is most clear at 100 km, at the end of the saltwater influence. There, the gravitational circulation almost vanishes, while the tidal ESCO circulation is still considerable. The tidal ESCO circulation can still establish itself, because other mechanisms than SIPS result in an M_2 eddy viscosity component. At 5 and 16 km, the indirect interactions make a particularly large contribution to the tidal ESCO circulation, which likely explains why this is the dominant exchange flow contribution there. At 56 km, the salinity gradient has its maximum absolute value, resulting in a dominant contribution of the exchange flow forced by the baroclinic pressure.

The tidal ESCO circulation induced by the external M_4 tide consistently has an opposite direction to the total exchange flow. It is also relatively large compared to the tidal ESCO circulation induced by the M_2 tide, considering that the tidal M_4 velocity is more than 10 times smaller than the tidal M_2 velocity. The M_4 tide mainly induces an exchange flow through the direct interaction with the M_4 eddy viscosity component. Since the M_4 eddy viscosity is relatively large, this interaction results in a relatively large exchange flow contribution. The M_4 eddy viscosity component is mainly induced by the M_2 tide, so the direction of the tidal ESCO due to the M_4 tide depends essentially on the phase difference between the M_2 and M_4 tide.

The exchange flow induced by momentum advection is relatively unimportant throughout the Scheldt River estuary. Only close to the mouth, it contributes about 8% to the exchange flow. It is expected that this contribution is more important in estuaries with a stronger width or depth convergence [see e.g., *Burchard et al*., 2014]. Strikingly, the advective ESCO circulation is negligible. This does not mean there are no direct or indirect interactions between the advection forcing and the temporally varying eddy viscosity. Rather, the exchange flow contributions induced by various interactions cancel against each other. The exact dependencies of the advective ESCO circulation on the amplitude and phase of the eddy viscosity differ from those of the gravitational ESCO circulation. This is because momentum advection induces different interactions with the eddy viscosity than the baroclinic forcing term.

The exchange flow contribution marked as "other" includes the vertical velocity variations of the tidal return flow and the river discharge, with the tidal return flow being much more important than the river discharge in this case. It is important to note that the depth-mean values of the river discharge and tidal return flow are not counted as exchange flow, see equation (17). ESCO also affects the exchange flow due to the river discharge and tidal return flow, by altering these vertical variations of the velocity profile. Depending on the location along the estuary, these contributions marked as "other" can be considerable or even dominant. Although often not considered when discussing exchange flows, these contributions should thus be taken into account.

7. Conclusion

In this paper, we have investigated the importance of various mechanisms in generating exchange flows by eddy viscosity-shear covariance (ESCO) using both a water column (1DV) and a width-averaged (2DV) model. Originally, the ESCO circulation is attributed to interactions between the M_2 tidal flow and the M_2 eddy viscosity caused by strain-induced periodic stratification (SIPS) [e.g., *Jay and Musiak*, 1994; *Burchard and Hetland*, 2010; *Burchard et al*., 2011; *Geyer and MacCready*, 2014]. Here we have shown that this *direct M_2–M_2 interaction* only explains a part of the total ESCO circulation. We emphasize the importance of other components of the velocity and of the time-varying eddy viscosity, including the M_2 eddy viscosity induced by other mechanisms than SIPS and the M_4 eddy viscosity component.

From a systematic analysis using a 1DV model, we have identified the *gravitational ESCO circulation*. This amplification of the gravitational circulation is caused by indirect interactions between the gravitational

circulation and the time-varying eddy viscosity. The dominant interaction is a two-step interaction, where the gravitational circulation interacts with the time-varying eddy viscosity to create time-varying velocity components. These components again interact with the time-varying eddy viscosity to create an amplification to the gravitational circulation. The interaction with the M_4 eddy viscosity component is especially important, since the M_4 eddy viscosity amplitude is generally large in estuaries with a predominant M_2 tide. The gravitational ESCO circulation has the same direction as the gravitational circulation, regardless of the phase of the eddy viscosity components. It is therefore a very robust mechanism for generating exchange flows. Typical parameter values for some Western European estuaries and tidal inlets provided by *Burchard et al*. [2013] are in the range where the gravitational ESCO circulation has a similar magnitude as the gravitational circulation and the tidal ESCO circulation.

We have also identified the contribution of indirect interactions to the tidal ESCO circulation. There is a multitude of relevant interactions that involve any component of the time-varying eddy viscosity. Each of these interactions can be as important as the direct M_2–M_2 interaction but can as well be oppositely directed. *Stacey et al*. [2008] already showed that the direction of the tidal ESCO circulation depends strongly on the moment of onset of stratification. This argument may be generalized by stating that the strength and direction of the tidal ESCO circulation depends on the relative amplitude and phase of all eddy viscosity components. Since the time-varying eddy viscosity is generated by a multitude of physical mechanisms, it is hard to make an a priori estimate of even the direction of the tidal ESCO circulation. In dominantly M_2 tidal systems with a weak M_2 eddy viscosity component, the direct M_2–M_2 interactions dominate any indirect interactions. Indirect interactions involving the M_4 eddy viscosity component become relatively more important for larger M_2 eddy viscosity amplitudes. The relative phase and strength of the M_4 eddy viscosity then also affect the strength and direction of the tidal ESCO circulation.

The width-averaged (2DV) case of the Scheldt River estuary demonstrates how the composition of the ESCO circulation varies over the distance along an estuary. It also demonstrates the importance of sources of time-varying turbulence other than SIPS. In the mixing zone between salt and fresh water, the relative strength of the tidal and gravitational ESCO circulation not simply is related to the salinity gradient but also strongly depends on the relative M_2 and M_4 eddy viscosity amplitude and phase. As a result, both contributions to the ESCO circulation are important at different locations. Both ESCO contributions and the gravitational circulation are of a similar order of magnitude in the saltwater zone. Assuming that the idealized model is at least indicative for the exchange flow in the Scheldt River estuary, this shows that the contribution by gravitational ESCO circulation cannot be ignored in real estuaries. In the freshwater zone, the gravitational ESCO circulation and gravitational circulation disappear, but the tidal ESCO circulation still persists. This is due to M_2 eddy viscosity contributions by e.g., tidal asymmetry, asymmetric shear, and depth variations with an M_2 tidal frequency.

The width-averaged case also demonstrates that the theory of exchange flows induced by indirect interactions can be generalized to other mechanisms. Basically, each term in the 3-D momentum budget equations could be associated with a direct generation mechanism for estuarine circulation and a respective ESCO term. Each forcing mechanism generates a contribution to the ESCO circulation with a different parameter dependency, which can be identified by a systematic analysis of the indirect interactions between the time-varying eddy viscosity and velocity shear. Such an analysis explains for example why the advective ESCO circulation is almost zero at a location where the gravitational ESCO circulation is important. Although not demonstrated here, there is no reason why the advective ESCO circulation could not be a dominant contribution to the exchange flow in other estuaries. Also not shown here is the important role of lateral circulation for the estuarine circulation, which has been highlighted by many studies during the last decade [*Lerczak and Geyer*, 2004; *Scully et al*., 2009; *Burchard et al*., 2011]. The strong direct contribution of lateral circulation to ESCO has been analyzed in detail by *Burchard and Schuttelaars* [2012]. Also, the wind stress has been shown to directly contribute to ESCO as discussed by *Burchard and Hetland* [2010].

Given these various contributions to ESCO, the earlier used expressions *tidal straining circulation* [e.g., *Burchard and Hetland*, 2010] or *asymmetric tidal mixing* [e.g., *Cheng et al*., 2011] are incomplete, since they only refer to particular components of the residual circulation generated by the *eddy viscosity-shear covariance* (ESCO). We therefore propose to use the more suitable expression *ESCO circulation*.

Acknowledgments
The authors are grateful to Deltares for hosting the major part of this research and to Rob Uittenbogaard, Jan van Kester, and Julie Pietrzak for their comments and suggestions. We also thank two anonymous reviewers for their constructive comments. We thank Valle-Levinson for helping to establish the term ESCO and we thank the many researchers that participated in a discussion on the ESCO terminology. The data used in this paper are listed in the references, tables, and figures.

References

Baumert, H., and G. Radach (1992), Hysteresis of turbulent kinetic energy in nonrotational tidal flows: A model study, *J. Geophys. Res.*, *97*, 3669–3677.

Brouwer, R. L., G. P. Schramkowski, T. Verwaest, and F. Mostaert (2015), Geïdealiseerde proceprocess van systeemovergangen naar hypertroebelheid. WP 1.3 Basismodel getij en zout [in Dutch], *Tech. Rep.* WL2015R13_103_3, Waterbouwkundig Lab. Borgerhout/Flanders Hydraul. Res., Antwerp, Belgium.

Burchard, H. (2009), Combined effects of wind, tide, and horizontal density gradients on stratification in estuaries and coastal seas, *J. Phys. Oceanogr.*, *39*, 2117–2136, doi:10.1175/2009JPO4142.1.

Burchard, H., and R. D. Hetland (2010), Quantifying the contributions of tidal straining and gravitational circulation to residual circulation in periodically stratified tidal estuaries, *J. Phys. Oceanogr.*, *40*, 1243–1262.

Burchard, H., and H. M. Schuttelaars (2012), Analysis of tidal straining as driver for estuarine circulation in well-mixed estuaries, *J. Phys. Oceanogr.*, *42*, 261–271, doi:10.1175/JPO-D-11-0110.1.

Burchard, H., R. D. Hetland, E. Schulz, and H. M. Schuttelaars (2011), Drivers of residual estuarine circulation in tidally energetic estuaries: Straight and irrotational channels with parabolic cross section, *J. Phys. Oceanogr.*, *41*, 548–570.

Burchard, H., H. M. Schuttelaars, and W. R. Geyer (2013), Residual sediment fluxes in weakly-to-periodically stratified estuaries and tidal inlets, *J. Phys. Oceanogr.*, *43*, 1841–1861.

Burchard, H., E. Schulz, and H. M. Schuttelaars (2014), Impact of estuarine convergence on residual circulation in tidally energetic estuaries and inlets, *Geophys. Res. Lett.*, *41*, 913–919, doi:10.1002/2013GL058494.

Chant, R. J. (2002), Secondary circulation in a region of flow curvature: Relationship with tidal forcing and river discharge, *J. Geophys. Res.*, *107*(C9), 3131, doi:10.1029/2001JC001082.

Chatwin, P. C. (1976), Some remarks and on the maintenance and of the and salinity distribution and in estuaries, *Estuarine Coastal Mar. Sci.*, *4*, 555–566.

Cheng, P., A. Valle-Levinson, and H. E. De Swart (2010), Residual currents induced by asymmetric tidal mixing in weakly stratified narrow estuaries, *J. Phys. Oceanogr.*, *40*, 2135–2147, doi:10.1175/2010JPO4314.1.

Cheng, P., A. Valle-Levinson, and H. E. De Swart (2011), A numerical study of residual circulation induced by asymmetric tidal mixing in tidally dominated estuaries, *J. Geophys. Res.*, *116*, C01017, doi:10.1029/2010JC006137.

Cheng, P., H. E. De Swart, and A. Valle-Levinson (2013), Role of asymmetric tidal mixing in the subtidal dynamics of narrow estuaries, *J. Geophys. Res. Oceans*, *118*, 2623–2639, doi:10.1002/jgrc.20189.

Chernetsky, A. S., H. M. Schuttelaars, and S. A. Talke (2010), The effect of tidal asymmetry and temporal settling lag on sediment trapping in tidal estuaries, *Ocean Dyn.*, *60*, 1219–1241, doi:10.1007/s10236-010-0329-8.

De Boer, G. J., J. D. Pietrzak, and J. C. Winterwerp (2008), Using the potential energy anomaly equation to investigate tidal straining and advection of stratification in a region of freshwater influence, *Ocean Modell.*, *22*, 1–11, doi:10.1016/j.ocemod.2007.12.003.

Deltares (2014), *Delft 3D User Manual, Version 3.15.34158*, Delft, Netherlands.

Dijkstra, Y. M., R. E. Uittenbogaard, J. A. T. M. Van Kester, and J. D. Pietrzak (2016), Improving the numerical accuracy of the $k-\varepsilon$ model by a transformation to the $k-\tau$ model, *Ocean Modell.*, *104*, 129–142.

Dijkstra, Y. M., et al. (2017), The iFlow modelling framework v2.4: A modular idealised processes model for flow and transport in estuaries, *Geosci. Model Dev.*, doi:10.5194/gmd-2017-20, in press.

Fischer, H. B. (1972), Mass-transport mechanisms in partially stratified estuaries, *J. Fluid Mech.*, *53*, 671–687, doi:10.1017/S0022112072000412.

Geyer, W. R., and P. MacCready (2014), The estuarine circulation, *Annu. Rev. Fluid Mech.*, *46*, 175–197, doi:10.1146/annurev-fluid-010313-141302.

Geyer, W. R., J. H. Trowbridge, and M. M. Bowen (2000), The dynamics of a partially mixed estuary, *J. Phys. Oceanogr.*, *30*, 2035–2048.

Hansen, D. V., and M. Rattray (1965), Gravitational circulation in straits and estuaries, *J. Mar. Res.*, *23*, 104–122.

Huijts, K. M. H., H. M. Schuttelaars, H. E. de Swart, and A. Valle-Levinson (2006), Lateral entrapment of sediment in tidal estuaries: An idealized model study, *J. Geophys. Res.*, *111*, C12016, doi:10.1029/2006JC003615.

IOC, SCOR, and IAPSO (2010), *The international thermodynamic equation of seawater 2010: Calculation and use of thermodynamic properties*. Intergovernmental Oceanographic Commission, Manuals and Guides No. 56, UNESCO (English), 196 pp.

Jay, D. A., and J. D. Musiak (1994), Particle trapping in estuarine tidal flows, *J. Geophys. Res.*, *99*, 20,445–20,461, doi:10.1029/94JC00971.

Lerczak, J. A., and W. R. Geyer (2004), Modelling the lateral circulation in straight, stratified estuaries, *J. Phys. Oceanogr.*, *34*, 1410–1428.

Li, C., and J. O'Donnell (2005), The effect of channel length on the residual circulation in tidally dominated estuaries, *J. Phys. Oceanogr.*, *35*, 1826–1840.

MacCready, P. (2004), Toward a unified theory of tidally-averaged estuarine salinity structure, *Estuaries*, *27*, 561–570, doi:10.1007/BF02907644.

Monismith, S. G., W. Kimmerer, J. R. Burau, and M. T. Stacey (2002), Structure and flow-induced and variability of the subtidal and salinity field and in and Northern San and Francisco Bay, *J. Phys. Oceanogr.*, *32*, 3003–3019.

Peters, H. (1999), Spatial and temporal variability of turbulent mixing in an estuary, *J. Mar. Res.*, *57*, 805–845.

Pritchard, D. W. (1956), The dynamic structure of a coastal plain estuary, *J. Mar. Res.*, *15*, 33–42.

Rippeth, T. P., N. R. Fischer, and J. H. Simpson (2001), The cycle of turbulent dissipation in the presence of tidal straining, *J. Phys. Oceanogr.*, *31*, 2458–2471.

Schulz, E., H. M. Schuttelaars, U. Gräwe, and H. Burchard (2015), Impact of the depth-to-width ratio of periodically stratified tidal channels on the estuarine circulation, *J. Phys. Oceanogr.*, *45*, 2048–2069.

Scully, M. E., C. T. Friedrichs, and J. M. Brubaker (2005), Control of estuarine stratification and mixing by wind-induced straining of the estuarine density field, *Estuaries*, *28*, 321–326.

Scully, M. E., W. R. Geyer, and J. A. Lerczak (2009), The influence of lateral advection on the residual estuarine circulation: A numerical modeling study of the Hudson River estuary, *J. Phys. Oceanogr.*, *39*, 107–124.

Simpson, J. H., J. Brown, J. Matthews, and G. Allen (1990), Tidal straining, density currents, and stirring in the control of estuarine stratification, *Estuaries*, *13*, 125–132, doi:10.2307/1351581.

Simpson, J. H., H. Burchard, N. R. Fischer, and T. P. Rippeth (2002), The semi-diurnal cycle of dissipation in a ROFI: model-measurement comparisons, *Cont. Shelf Res.*, *22*, 1615–1628.

Simpson, J. H., E. Williams, L. H. Brasseur, and J. M. Brubaker (2005), The impact of tidal straining on the cycle of turbulence in a partially stratified estuary, *Cont. Shelf Res.*, *25*, 51–64.

Stacey, M. T., and D. K. Ralston (2005), The scaling and structure of the estuarine bottom boundary layer, *J. Phys. Oceanogr.*, *35*, 55–71.

Stacey, M. T., J. P. Fram, and F. K. Chow (2008), Role of tidally periodic density stratification in the creation of estuarine subtidal circulation, *J. Geophys. Res.*, *113*, C08016, doi:10.1029/2007JC004581.

Uittenbogaard, R. E., J. A. T. M. Van Kester, and G. S. Stelling (1992), Implementation of three turbulence models in 3D-TRISULA for rectangular grids, *Tech. Rep. Z81*, WL, Delft Hydraul., Delft, Netherlands.

Van Aken, H. M. (1986), The onset of seasonal stratification in shelf seas due to differential advection in the presence of a salinity gradient, *Cont. Shelf Res.*, *5*, 475–485.

Verspecht, F., T. P. Rippeth, J. H. Simpson, A. J. Souza, H. Burchard, and M. J. Howarth (2009), Residual circulation and stratification in the Liverpool Bay region of freshwater influence, *Ocean Dyn.*, *59*, 765–779, doi:10.1007/s10236-009-0233-2.

Wei, X., G. P. Schramkowski, and H. M. Schuttelaars (2016), Salt dynamics and in well-mixed and estuaries: Importance and of advection and by tides, *J. Phys. Oceanogr.*, *46*, 1457–1475.